PROCEEDINGS OF SPIE

SPIEDigitalLibrary.org/conference-proceedings-of-spie

Compressed optoacoustic data acquisition based on a cluster of acoustic scatterers

X. L. Deán-Ben, A. Özbek, D. Razansky

X. L. Deán-Ben, A. Özbek, D. Razansky, "Compressed optoacoustic data acquisition based on a cluster of acoustic scatterers," Proc. SPIE 10878, Photons Plus Ultrasound: Imaging and Sensing 2019, 108781K (27 February 2019); doi: 10.1117/12.2510020



Event: SPIE BiOS, 2019, San Francisco, California, United States

Compressed optoacoustic data acquisition based on a cluster of acoustic scatterers

X. L. Deán-Ben^{1,2,3}, A. Özbek^{1,2,3} and D. Razansky^{1,2,3}
¹Faculty of Medicine and Institute of Pharmacology and Toxicology, University of Zurich,
Switzerland

²Institute for Biomedical Engineering and Department of Information Technology and Electrical Engineering, ETH Zurich, Switzerland

³Institute of Biological and Medical Imaging (IBMI), Technical University of Munich and Helmholtz Center Munich, Germany

ABSTRACT

A myriad of optoacoustic imaging systems based on scanning focused ultrasound transducers or on tomographic acquisition of pressure signals are available. In all cases, image formation is based on the assumption that ultrasound waves undergo no distortion and propagate with constant velocity across the sample and coupling medium (typically water). Thereby, ultrasound time-of-flight readings from multiple time-resolved signals are required to form an image. Acoustic scattering is known to cause distortion in the signals and is generally to be avoided. In this work, we exploit acoustic scattering to physically encode the position of optical absorbers in the acquired time-resolved signals and hence reduce the amount of data required to reconstruct an image. This new approach was experimentally tested with an array of cylindrically-focused transducers, where a cluster of acoustic scatterers was introduced in the ultrasound propagating path between the sample and the array elements. Ultrasound transmission was calibrated by raster scanning a light-absorbing particle across the effective field of view. The acquired calibrating signals were then used for the development of a regularized model-based iterative algorithm that enabled reconstructing an image from a relatively low number of optoacoustic signals. A relatively short acquisition time window was needed to capture the entire optoacoustic field, which demonstrates the high signal compression efficiency. The feasibility to form an image with a relatively low number of signals is expected to play a major role in the development of a new generation of optoacoustic imaging systems.

Keywords: Optoacoustic tomography, Compressed-sensing, Acoustic scattering, Time-resolved signals.

1. INTRODUCTION

Optoacoustic (OA, photoacoustic) imaging takes advantage of the low scattering of ultrasound waves relative to light in biological tissues to render high-resolution images at depths well-beyond the light diffusion limit [1,2]. Optical contrast (absorption) mapping is achieved based on ultrasound time-of-flight readings from multiple time-resolved signals acquired by either scanning a single-element transducer or by using a transducer array. Multiple types of ultrasound transducers and scanning geometries have been suggested in a myriad of OA tomographic embodiments to image small animals and selected areas in humans [3-8]. In all these systems, image formation is based on the assumption that ultrasound waves undergo no distortion and propagate with constant velocity across the sample and coupling medium (typically water). However, acoustic reflections or acoustic scattering may take place at internal structures within the sample. These phenomena are generally undesirable as they can severely deteriorate the images obtained with standard reconstruction methods [9-11].

Acoustic reflections and scattering generally lead to the appearance of late responses in the time-resolved signals collected at different positions, which are known to be the cause of arc-type artefacts in OA images [12]. However, late signal responses can contain useful information to be used for image formation. For example, acoustic reflectors (mirrors) have been included in OA tomographic imaging systems based on linear or planar arrays to be able to acquire

Photons Plus Ultrasound: Imaging and Sensing 2019, edited by Alexander A. Oraevsky, Lihong V. Wang, Proc. of SPIE Vol. 10878, 108781K \cdot © 2019 SPIE \cdot CCC code: 1605-7422/19/\$18 \cdot doi: 10.1117/12.2510020

the pressure signals at the "virtual detector" locations [13]. This effectively doubles the information contained in each acquisition and enables maximizing the effective angular coverage and so avoid so-called limited-view effects [14]. Indeed, multiple OA signals are required to trilaterate the location of optical absorbers, and the additional information associated to acoustic reflections can effectively reduce the number of signals required. The location of an absorber can potentially be encoded in a single time-resolved signal if a sufficient number of reflected waves are acquired, for which a relatively large acquisition window is needed.

In this work, we suggest a method to encode the spatial location of optical absorbers in time-resolved OA signals based on multiple scattering of ultrasound waves. For this, randomly distributed acoustic scatterers are placed in front of a transducer array, which provide a distinctive ultrasound propagation path for the waves generated at each point of the region of interest. As a consequence, the number of signals required for OA reconstructing can be significantly reduced without considerably enlarging the acquisition time window.

2. MATERIALS AND METHODS

2.1 Experimental set-up

A lay-out of the experimental system used to test the suggested approach is depicted in Fig. 1a. Basically, a full-ring (\sim 360°) array of cylindrically-focused transducers was employed to collect the OA signals generated by directly illuminating a light-absorbing sample located within the focal plane. The custom-made detector array (Imasonic SaS, Voray, France) consists of two concave sub-arrays with 256 elements each (512 elements in total). Each sub-array has active angular aperture of 174°, a radius of curvature of 40 mm, a focal distance of 38 mm and an inter-element pitch of 0.47 mm [15]. The detection elements have a central frequency of 5 MHz and >80% detection bandwidth. The dimensions of the elements are $0.37x15 \text{ mm}^2$. Illumination was provided with an optical parametric oscillator (OPO)-based laser (Innolas GmbH, Krailling, Germany) operating at a pulse repetition of 100 Hz and tuned to 720 nm to achieve maximum energy per pulse.

A cluster of acoustic scatterers were randomly distributed along a circular ring coaxially-aligned with the array (Fig. 1c). Specifically, ~300 borosilicate capillary glass tubings with inside and outside diameters of 0.86 and 1.50 mm respectively (Warner Instruments LLC, Hamden, USA) were distributed along an annulus with 16 mm radius and 20 mm thickness. The effects of acoustic scattering in the collected OA signals are illustrated in Figs. 1b and 1d. Fig. 1b shows the OA signal corresponding to a ~100 μ m polyethylene microsphere (Cospheric LLC, Santa Barbara, USA) being acquired with a transducer element of the array with no scatterers in the propagating path. It is shown that the signal is confined in time to a small interval $\Delta t_1 \sim 1/BW$ centered at t=d/c, being BW the detection bandwidth, d the distance between the sphere and the sensor and c the speed of sound. Fig. 1d displays the signal acquired with a high density of scatterers in the ultrasound propagating path equivalent to that in the experimental set-up. This signal exhibits a complex pattern expanding for $\Delta t_2 \sim 10 \,\mu$ s with no dominant peaks, in a way that all sampling instants within Δt_2 contain information on the location of the OA point source.

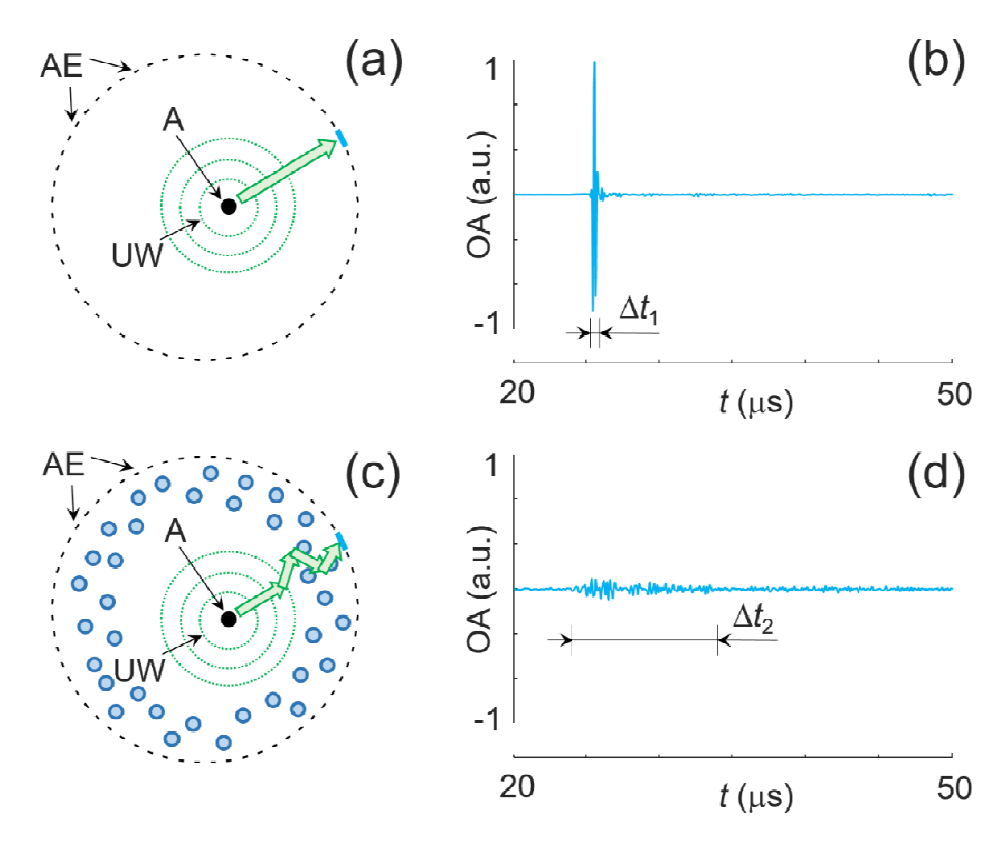


Figure 1: Schematic representation of the suggested imaging system. (A) Lay-out of the full-ring transducer array. AE – array elements, A – absorber, UW – ultrasound waves. (b) Time-resolved signal acquired by an array element for direct propagation of the ultrasound wave (no scattering). (c) Modification of the set-up to include a cluster of acoustic scatterers (blue circles). (d) Time-resolved signal acquired by the same array element as in (b) for waves undergoing multiple scattering events in the propagating path.

2.2 System calibration and reconstruction method

Image reconstruction in the presence of acoustic scattering implies developing a model relating the initial OA pressure, which is proportional to optical absorption, to the collected time-resolved pressure signals. In the same manner as in model-based OA reconstruction approaches in the time domain [16,17,18], it is reasonable to assume that the absorbed energy is confined within the region of interest (ROI) and that the acquired OA signals p(r,t) correspond to a linear superposition of the signals $p_i(r,t)$ for each pixel of a grid covering such ROI, i.e.,

$$p(r,t) = \sum_{i} h_i p_i(r,t), \tag{1}$$

where h_i are the pixel intensities. When acoustic scattering takes place, the derivation of a theoretical model for $p_i(r,t)$ becomes very challenging. Alternatively, $p_i(r,t)$ can be experimentally measured by placing an OA source at a grid of points and collecting the corresponding responses. This was achieved by scanning a ~100 μ m polyethylene microsphere for a ROI of 4.5x4.5 mm² (75 μ m step). Based on the measured signals, Eq. (1) can be expressed in a matrix form as

$$\mathbf{p} = \mathbf{MH},\tag{2}$$

where p is a column vector containing the signal(s) for a set of measuring positions and instants and H is a vector containing the pixel intensities of the scanning grid. M is the model matrix, whose columns are the signal(s) acquired for each position of the scanned particle, or alternatively, a linear superposition of those. Tomographic reconstruction of an OA from the acquired signals p_m can be performed via

$$\mathbf{H}_{\text{sol}} = \operatorname{argmin}_{\mathbf{H}} \{ \|\mathbf{p}_{\text{m}} - \mathbf{M}\mathbf{H}\|_{2}^{2} + \lambda^{2} \|\mathbf{H}\|_{l}^{2} \},$$
 (3)

where the parameter λ allows weighting the regularization term $\|\mathbf{H}\|_{L}^{2}$, with l=1 or l=2.

2.3 Experimental measurements

The feasibility to reconstruct an image with the suggested approach was tested with a $\sim 100 \, \mu m$ polyethylene microsphere scanned at random points within the ROI not included in the calibration grid. The 512 OA signals of all array elements were digitized at 40 megasamples per second for a time window of 494 samples delayed by 20 μs with respect to the emission of the laser pulse. The matrix M was built by considering a single time-resolved signal was considered corresponding to the sum of the signals from all array elements, and the reconstructions were accordingly performed.

3. RESULTS

Exemplary results obtained for the experiments described in section 2.3 are displayed in Fig. 2. Specifically, the reconstructions rendered for a single microparticle and for a distribution of three microparticles are displayed in the left and right columns, respectively. The results obtained with L2-norm-based regularization (l=2 in Eq. 3) are shown in Figs. 2a and 2b, while the equivalent results obtained with L1-norm-based regularization (l=1 in Eq. 3) are displayed in Figs. 2c and 2d. It is shown that the width of the reconstructed microparticles is lower when using the L1 norm. However, this must not be ascribed to a higher spatial resolution but rather to the sparsity conditions imposed. It is also shown that noisier images are rendered when reconstructing several microparticles. Indeed, OA reconstruction from a single signal becomes challenging when reducing the sparsity of the images, and accurate results could not be achieved for a larger number of microparticles.

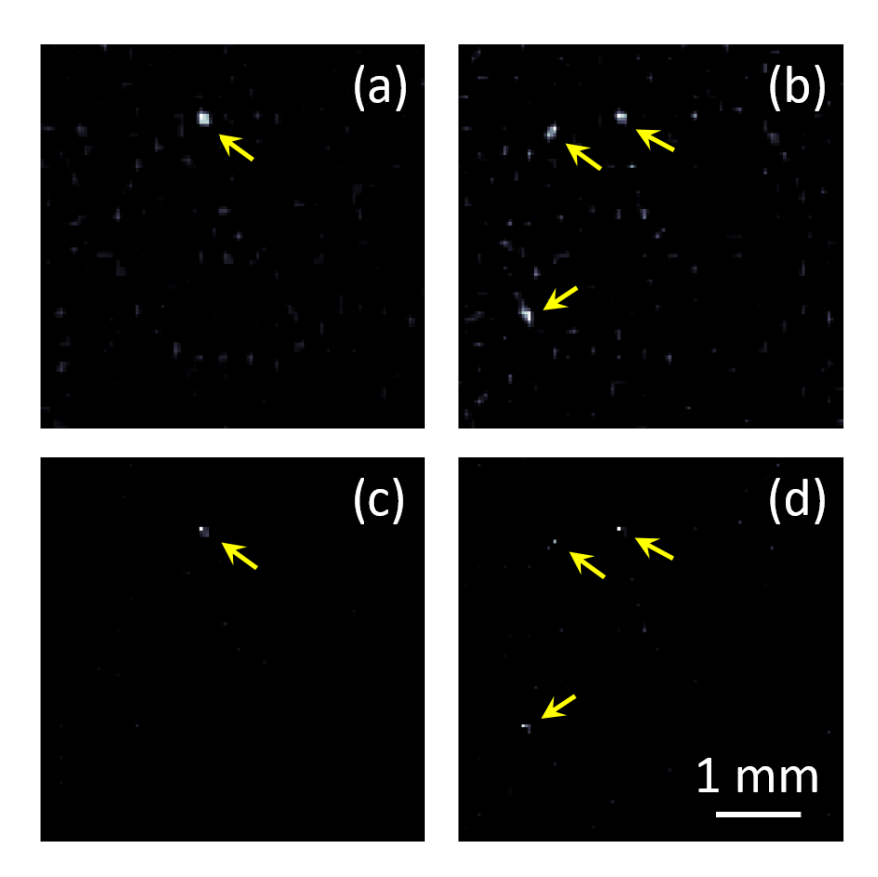


Figure 2: Tomographic reconstructions for $\sim 100 \, \mu m$ polyethylene microsphere located at different positions. (a-b) Images obtained when considering a regularization term based on the L2 norm (l=2 in Eq. 3). (c-d) Images obtained when considering a regularization term based on the L1 norm (l=1 in Eq. 3). Yellow arrows indicate the position of the particles.

4. DISCUSSION AND CONCLUSIONS

The presented results demonstrate that it is possible to minimize the amount of data required for OA image formation via "physically" encoding the optical absorption distribution in a defined ROI in a single time-resolved signal. This is essential for advancing on the capabilities of this continuously growing technology and to reduce costs in order to make it more accessible worldwide. Herein, we have capitalized on the complex propagation path of ultrasound waves in a scattering medium. Thus, while several time-of-flight readings are generally required to reconstruct the position of a given OA source, the approach suggested in this work retrieves this information from multiple time samples of the acquired scattered wave. An OA system based on compressed data acquisition can significantly enhance the dynamic imaging performance [19]. In principle, the time resolution in OA is ultimately limited by the unidirectional propagation of ultrasound through the ROI. This ultimate limit may not be reached with the suggested approach due to the fact that the acquisition time window needs to be enlarged to capture the scattered field.

It is also important to highlight that a potential drawback of the suggested approach relates to the fact that sparsity is generally needed for OA image reconstruction. We have shown than a single absorber can be very accurately reconstructed with a single signal, but this becomes more challenging for multiple sources. Reconstruction of sparsely distributed absorbers is important in localization OA tomography (LOT) [20,21] or methods based on image fluctuations [22,23] that can break through the acoustic diffraction barrier. i.e., the suggested methodology may find applicability for super-resolution imaging of vascular structures. On the other hand, a similar approach to achieve pulse-echo ultrasound images with a single signal has been suggested [24]. Thereby, hybrid OA and pulse-echo ultrasound imaging may as well

be possible, which is highly important for the clinical translation of the OA technology [25,26]. Overall, the feasibility to form an image with a single time-resolved signal is expected to play a major role in the development of cheaper, faster and more efficient OA imaging systems.

REFERENCES

- [1] Wang, L. V. and Hu, S., "Photoacoustic tomography: in vivo imaging from organelles to organs," Science 335(6075), 1458-1462 (2012).
- [2] Dean-Ben, X. L., et al., "Advanced optoacoustic methods for multiscale imaging of in vivo dynamics," Chemical Society Reviews 46(8), 2158-2198 (2017).
- [3] Razansky, D. et al., "Volumetric real-time multispectral optoacoustic tomography of biomarkers," Nature Protocols 6(8), 1121 (2011).
- [4] Jathoul, A. P. et al., "Deep in vivo photoacoustic imaging of mammalian tissues using a tyrosinase-based genetic reporter Fresnel lenses in rear projection displays," Nature Photonics 9(4), 239 (2015).
- [5] Ermilov, S. A. et al., "Three-dimensional optoacoustic and laser-induced ultrasound tomography system for preclinical research in mice: design and phantom validation Fresnel lenses in rear projection displays," Ultrasound Imaging 38(1), 77-95 (2016).
- [6] Fehm, T. F. et al., "In vivo whole-body optoacoustic scanner with real-time volumetric imaging capacity," Optica 3(11), 1153-1159 (2016).
- [7] Dean-Ben, X. L. et al., "Spiral volumetric optoacoustic tomography visualizes multi-scale dynamics in mice," Light: Science & Applications 6(4), e16247 (2017).
- [8] Li, L. et al, "Single-impulse panoramic photoacoustic computed tomography of small-animal whole-body dynamics at high spatiotemporal resolution," Nature Biomedical Engineering 1(5), 0071 (2017).
- [9] Dean-Ben, X. L. et al., "Statistical approach for optoacoustic image reconstruction in the presence of strong acoustic heterogeneities Fresnel lenses in rear projection displays," IEEE Transactions on Medical Imaging 30(2), 401-408 (2011).
- [10] Dean-Ben, X. L. et al., "Weighted model-based optoacoustic reconstruction in acoustic scattering media," Physics in Medicine & Biology 58(16), 5555 (2013).
- [11] Poudel, J. et al., "Mitigation of artifacts due to isolated acoustic heterogeneities in photoacoustic computed tomography using a variable data truncation-based reconstruction method," Journal of Biomedical Optics 22(4), 041018 (2017).
- [12] Dean-Ben, X. L. et al., "Artefact reduction in optoacoustic tomographic imaging by estimating the distribution of acoustic scatterers," Journal of Biomedical Optics 17(11), 110504 (2012).
- [13] Huang, B. et al., "Improving limited-view photoacoustic tomography with an acoustic reflector," Journal of Biomedical Optics 18(11), 110505 (2013).
- [14] Dean-Ben, X. L. et al., "On the link between the speckle free nature of optoacoustics and visibility of structures in limited-view tomography," Photoacoustics 4(4), 133-140 (2016).
- [15] Mercep, E.., "Transmission-Reflection Optoacoustic Ultrasound (TROPUS)," Light: Science & Applications (in press).
- [16] Paltauf, G. et al., "Iterative reconstruction algorithm for optoacoustic imaging," Journal of the Acoustical Society of America 112(4), 1536-1544 (2002).
- [17] Rosenthal, A. et al., "Fast semi-analytical model-based acoustic inversion for quantitative optoacoustic tomography," IEEE Transactions on Medical Imaging 29(6), 1275-1285 (2010).
- [18] Ding, L. et al., "Real-time model-based inversion in cross-sectional optoacoustic tomography," IEEE Transactions on Medical Imaging 35(8), 1883-1891 (2016).
- [19] Özbek, A. et al., "Optoacoustic imaging at kilohertz volumetric frame rates," Optica 5(7), 857-863 (2018).
- [20] Vilov, S. et al., "Overcoming the acoustic diffraction limit in photoacoustic imaging by the localization of flowing absorbers," Optics Letters 42(21), 4379-4382 (2017).
- [21] Dean-Ben, X. L. and Razansky, D., "Localization optoacoustic tomography," Light: Science & Applications 7(4), 18004 (2018).

- [22] Dean-Ben, X. L. et al., "Dynamic particle enhancement in limited-view optoacoustic tomography," Optics Letters 42(4), 827-830 (2017).
- [23] Chaigne, T. et al., "Super-resolution photoacoustic imaging via flow-induced absorption fluctuations," Optica 4(11), 1397-1404 (2017).
- [24] Kruizinga, P. et al, "Compressive 3D ultrasound imaging using a single sensor," Science Advances 3(12), e17011423 (2017).
- [25] Kim, J. et al., "Programmable real-time clinical photoacoustic and ultrasound imaging system," Scientific Reports 6, 35137 (2016).
- [26] Mercep, E. et al., "Combined pulse-echo ultrasound and multispectral optoacoustic tomography with a multisegment detector array," IEEE Transactions on Medical Imaging 36(10), 2129-2137 (2017).